Error Rate Analysis for Peaky Signaling over Fading Channels[1]

Mustafa Cenk Gursoy
Department of Electrical Engineering
University of Nebraska-Lincoln, Lincoln, NE 68588
Email: gursoy@engr.unl.edu

Abstract

In this paper, the performance of signaling strategies with high peak-to-average power ratio is analyzed over both coherent and noncoherent fading channels. Two modulation schemes, namely on-off phase-shift keying (OOPSK) and on-off frequency-shift keying (OOFSK), are considered. Initially, uncoded systems are analyzed. For OOPSK and OOFSK, the optimal detector structures are identified and analytical expressions for the error probabilities are obtained for arbitrary constellation sizes. Numerical techniques are employed to compute the error probabilities. It is concluded that increasing the peakedness of the signals results in reduced error rates for a given power level and hence equivalently improves the energy efficiency for fixed error probabilities. The coded performance is also studied by analyzing the random coding error exponents achieved by OOPSK and OOFSK signaling.

Index Terms: Peaky signaling, Maximum a-posteriori probability (MAP) detection, error probability, on-off keying, phase-shift keying, frequency-shift keying, random coding error exponents.

I. Introduction

In wireless communications, when the receiver and transmitter have only imperfect knowledge of the channel conditions, efficient transmission strategies have a markedly different structure than those employed over perfectly known channels. For instance, Abou-Faycal *et al.* [1] studied the noncoherent Rayleigh fading channel where the receiver and transmitter has no channel side information, and showed that the capacity-achieving input amplitude distribution is discrete with a finite number of mass points. It has also been shown that there always exists a mass point at the origin. These results indicate that unlike perfectly known channels where a Gaussian input is optimal and a continuum of amplitude levels are available for tranmission, only

This work was supported in part by the NSF CAREER Grant CCF-0546384. The material in this paper was presented in part at the 40th Annual Asilomar Conference on Signals, Systems, and Computers, Nov. 2006, and the 40th Annual Conference on Information Sciences and Systems, Princeton University, Princeton, NJ, March, 2006.

finitely many amplitude levels with one level at the origin should be used for transmission over noncoherent Rayleigh channels. The discreteness of the optimal amplitude distribution has also been shown over other noncoherent channels (see e.g., [2], [3], [4], [6], and references therein).

Another key result for noncoherent channels is the requirement of transmission with high peak-to-average power ratio in the low signal-to-noise ratio (SNR) regime. In noncoherent Rayleigh channels [1], the optimal amplitude has two mass points for low SNR values, and the nonzero mass migrates away from the origin, increasing the peak power, as SNR decreases. Indeed, this behavior has been shown in a more general setting in [5] where *flash signaling* is proven to be the necessary form of transmission to achieve the capacity of imperfectly-known fading channels in the low-SNR regime.

The impact upon the channel capacity of using signals with limited peakedness is investigated in [7], [8], [9], and [10]. In [7], two types of signaling schemes are defined: on-off binary phase-shift keying (OOBPSK) and on-off quaternary phase-shift keying (OOQPSK). These modulations are obtained by overlaying on-off keying on phase-shift keying. The peakedness of these signals are controlled by changing the probability of no transmission. OOQPSK is shown to be an optimally efficient modulation scheme for transmission over noncoherent Rician fading channels in the low-SNR regime. In [18], the capacity and power efficiency of another type of peaky signaling scheme, on-off frequency-shift keying (OOFSK), have been studied in Rician fading channels with perfect or imperfect channel information at the receiver. Note that OOFSK introduces peakedness in both time and frequency.

The aforementioned studies have focused on the achievable rates and channel capacity. Recently, there have also been interest in the error performance in noncoherent fading channels. Reference [13] considered the error exponents and cutoff rate of noncoherent Rician fading channels and showed that the optimal input again has a discrete structure. Huang *et al* [14] proved, under more general assumptions on the channel, the discreteness of the input that achieves the optimal random coding error error exponent. Wu and Srikant [15] considered multiple-input multiple-output (MIMO) fading channels and characterized the reliability function in the low-SNR regime. They analyzed the relation between the communication rate, error exponents, number of antennas, and signal peakiness. Ray *et al.* [16] analyzed the capacity and the random coding error exponents of noncoherent Rayleigh MIMO fading channels in the wideband regime in which the SNR per degree of freedom is low and coherence length is large. Lun *et al.* [12] also investigated the error

probabilities of peaky signaling. They considered peaky FSK modulation and characterized the reliability function in the infinite bandwidth regime. Luo *et al.* [11] introduced multitone FSK schemes and obtained upper and lower bounds on the probability of error of these signaling schemes over wideband noncoherent Rayleigh fading channels.

The above-mentioned studies mainly analyze the error probability of coded systems in noncoherent fading channels by considering the error exponents. Generally, the analysis is performed in the low-SNR regime. [13] and [14] consider general SNR levels but focus on the structure of the input distribution that achieves the maximum error exponents. In this paper, we present a different approach. Our contributions are the following. We consider two particular peaky modulation schemes: on-off phase-shift keying (OOPSK) and on-off frequency-shift keying (OOFSK). We determine the optimal detector structures and analyze the error probabilities of uncoded OOPSK and OOFSK. The analysis is conducted for both coherent and noncoherent fading channels, and error performances are investigated at low-to-high SNR levels. We find that the error performance of signaling with high peak-to-average power ratio is superior to that of conventional PSK and FSK modulations over the entire SNR range if the duty cycles of modulations are small enough. Equivalently, peaky signaling is shown to be more energy efficient for fixed error probabilities. We have also considered the coded performance by obtaining the error exponents of OOPSK and OOFSK modulations. As a result of the analysis conducted in this paper, information-theoretic inspired signaling schemes, OOPSK and OOFSK, emerge as energy efficient modulation formats especially well-suited for low data rate applications such as in sensor networks.

The rest of the paper is organized as follows. We describe the modulation techniques and the channel model in Section II. We study the error probabilities in coherent fading channels in Section III while the performance in noncoherent fading channels is analyzed in Section IV. We study the random coding error exponents of peaky signaling in Section V. Finally, Section VI includes our conclusions.

II. System Model

In this section, we present the system model. We consider two types of signaling at the transmitter side, OOPSK and OOFSK. Basically, these two modulation schemes are obtained by overlaying on-off keying on phase-shift keying and frequency-shift keying, respectively. In both signaling schemes, transmitter sends over the symbol interval of $[0, T]$ either no signal with probability $1 - \nu$ or one of M signals, each with

probability ν/M. The transmitted signal can be mathematically expressed as

$$s_i(t) = \begin{cases} \sqrt{\frac{P}{\nu}}\, e^{j(\omega_i t+\theta_i)} & 1 \le i \le M \quad \text{with prob. } \nu/M \\ 0 & i = 0 \qquad\quad \text{with prob. } (1-\nu) \end{cases} \qquad 0 \le t \le T \tag{1}$$

where P is the average power, ω_i and θ_i are the frequency in radians and phase of $s_i(t)$, respectively. $s_0(t) = 0$ denotes no transmission. In OOPSK modulation, the frequency is fixed, i.e., $\omega_i = \omega\ \forall i$, and phases are $\theta_i = \frac{2\pi(i-1)}{M}$ for $1 \le i \le M$. In OOFSK, information is carried by the frequencies and each nonzero signal has a distinct frequency. To ensure orthogonality, adjacent frequency slots satisfy $|\omega_{i+1} - \omega_i| = \frac{2\pi}{T}$. In OOFSK, phases can be arbitrary. In both modulations, ν can be regarded as the duty cycle of the transmission. Note also that both modulation formats have an average power of P and a peak power of $\frac{P}{\nu}$, and hence a peak-to-average power ratio (PAR) of $\frac{1}{\nu}$. Limitations on the PAR of the signaling scheme, which may be dictated by regulations or system component specifications, are reflected in the choice of the value of ν.

We assume that the transmitted signal undergoes stationary and ergodic fading and that the delay spread of the fading is much less than the symbol duration. Under this narrowband assumption, the fading has a multiplicative effect on the transmitted signal. If we further assume that the symbol duration T is less than the coherence time of the fading, then the fading stays constant over the symbol duration. Hence, if the transmitted signal is $s_i(t)$, the received signal is

$$r(t) = h_k\, s_i(t-(k-1)T) + n(t), \quad (k-1)T \le t \le kT, \qquad \text{for } i = 0, 1, 2, \ldots, M \text{ and } k = 1, 2, \ldots,$$

where $\{h_k\}$ denotes the sequence of fading coefficients and is a proper, complex, stationary, ergodic fading process with finite variance, and $n(t)$ is a zero-mean, circularly symmetric, white complex Gaussian noise process with single-sided spectral density N_0. The transmitted signal, fading coefficients, and additive noise are assumed to be mutually independent of each other.

If OOPSK modulation is used at the transmitter, the receiver demodulates the received signal using a correlator:

$$\begin{aligned} y_k &= \frac{1}{\sqrt{N_0 T}} \int_{(k-1)T}^{kT} r(t) e^{-j\omega(t-(k-1)T)} dt \qquad (2) \\ &= \frac{1}{\sqrt{N_0 T}} \int_0^T \left[h_k s_i(t) e^{-j\omega t} + n(t+(k-1)T) e^{-j\omega t} \right] dt = \begin{cases} \alpha h_k e^{j\theta_i} + n_k & 1 \le i \le M \\ n_k & i = 0 \end{cases} \quad k = 1, 2, 3 \ldots \end{aligned}$$

where $\alpha = \sqrt{\frac{PT}{\nu N_0}}$, $\theta_i = \frac{2\pi(i-1)}{M}$ for $1 \leq i \leq M$, and $\{n_k\}$ is a sequence of independent and identically distributed (i.i.d.) circularly symmetric complex Gaussian random variables with zero mean and variance $E\{|n_k|^2\} = 1$.

If OOFSK signals are transmitted, a bank of M correlators is employed at the receiver and the output of the m^{th} correlator at time $t = kT$ is given by:

$$y_{k,m} = \frac{1}{\sqrt{N_0 T}} \int_{(k-1)T}^{kT} r(t) e^{-j\omega_m (t-(k-1)T)} dt \tag{3}$$

$$= \frac{1}{\sqrt{N_0 T}} \int_0^T \left[h_k s_i(t) e^{-j\omega_m t} + n(t + (k-1)T) e^{-j\omega_m t} \right] dt \tag{4}$$

$$= \begin{cases} \alpha h_k e^{j\theta_i} + n_{k,m} & m = i \\ n_{k,m} & m \neq i \end{cases}, \quad m = 1, 2, \ldots, M, \quad i = 0, 1, \ldots, M \quad k = 1, 2, \ldots \tag{5}$$

where again $\alpha = \sqrt{\frac{PT}{\nu N_0}}$, and $\{n_{k,m}\}$ is an i.i.d sequence in both k and m of zero-mean unit-variance circularly symmetric complex Gaussian random variables. The output of M demodulators is denoted by the M-dimensional vector $\mathbf{y}_k = [y_{k,1}, y_{k,2}, \ldots, y_{k,M}]$.

III. Error Probability in Coherent Fading Channels

In this section, we assume that the receiver perfectly knows the instantaneous realizations of the fading coefficients $\{h_k\}$ whereas the transmitter has no such knowledge.

A. OOPSK

We first consider OOPSK signaling. For the detection of these signals, maximum a posteriori probability (MAP) decision rule, which minimizes the probability of error, is employed after demodulation at the receiver. It is assumed that symbol-by-symbol detection is performed, and henceforth we drop the time index k without loss of generality. In MAP detection, signal s_i is chosen as the detected signal if

$$p_i \, f_{y|s_i,h}(y|s_i, h) > p_j \, f_{y|s_j,h}(y|s_j, h) \quad \forall j \neq i \tag{6}$$

where p_i and p_j denote the prior transmission probabilities of the signals s_i and s_j, respectively, and

$$f_{y|s_i,h}(y|s_i, h) = \begin{cases} \frac{1}{\pi} e^{-|y - \alpha h e^{j\theta_i}|^2} & 1 \leq i \leq M \\ \frac{1}{\pi} e^{-|y|^2} & i = 0 \end{cases} \tag{7}$$

is the conditional probability density function of the output given s_i and h. Note from (1) that $p_i = \nu/M$ for $i \neq 0$ and $p_0 = 1 - \nu$. The following result provides the decision regions and the error probability for OOPSK modulation.

Proposition 1: The optimal decision regions for OOPSK signals when transmitted over coherent fading channels are

$$\mathcal{D}_i = \left\{ y = |y|e^{j\theta_y} : \frac{2\pi(i-\frac{3}{2})}{M} \leq \theta_y \leq \frac{2\pi(i-\frac{1}{2})}{M} \text{ and } |y|\cos(\theta_y - \theta_i) > \tau \right\} \quad 1 \leq i \leq M, \tag{8}$$

$$\mathcal{D}_0 = \left\{ y = |y|e^{j\theta_y} : |y|\cos(\theta_y - \theta_i) < \tau \quad \forall i \neq 0 \right\}, \tag{9}$$

where $\tau = \begin{cases} \zeta & \zeta \geq 0 \\ 0 & \zeta < 0 \end{cases}$ and $\zeta = \frac{\alpha|h|}{2} + \frac{1}{2\alpha|h|}\ln\left(\frac{M(1-\nu)}{\nu}\right)$. Moreover, the error probability as a function of the instantaneous realization of the fading magnitude, $|h|$, is

$$P_{e|\,|h|} = 1 - \left((1-\nu)P_{c|s_0,|h|} + \nu P_{c|s_1,|h|}\right), \tag{10}$$

where

$$P_{c|s_0,|h|} = M\int_0^{\tau}\left(1 - 2Q\left(\sqrt{2}x\tan\frac{\pi}{M}\right)\right)\frac{e^{-x^2}}{\sqrt{\pi}}\,dx \text{ and } P_{c|s_1,|h|} = \int_{\tau}^{\infty}\left(1 - 2Q\left(\sqrt{2}\,x\tan\frac{\pi}{M}\right)\right)\frac{e^{-(x-\alpha|h|)^2}}{\sqrt{\pi}}\,dx \tag{11}$$

are the correct detection probabilities when $s_0(t)$ and $s_1(t)$, respectively, are the transmitted signals.

Proof: Using the property that phase-shift keying signals have the same energy, the detection rule in (6) can easily be simplified to the following: The signal s_i for $i \neq 0$ is the detected signal if

$$\Re(ye^{-j\theta_i}) > \Re(ye^{-j\theta_j}) \quad \forall j \neq i, 0 \quad \text{and} \quad \Re(ye^{-\theta_i}) > \tau \tag{12}$$

where $\Re(z)$ is used to denote the real part of the complex scalar z, and τ is defined in the proposition above. No transmission is detected if

$$\Re(ye^{-j\theta_i}) < \tau \quad \forall i \neq 0. \tag{13}$$

Note that the phase θ_h of the fading coefficients has no effect on the error probability as long as the receiver, knowing perfectly the phase rotations introduced by the channel, removes any phase offset by

using $\tilde{y} = ye^{-\theta_h}$ at the detector. Hence, the detection rules (12) and (13) are obtained by assuming without loss of generality that $\theta_h = 0$ and hence $h = |h|$. These detection rules lead to the decision regions given in the proposition. After the identification of the decision regions, performance analysis is easily conducted. The correct detection probabilities in (11) are obtained from

$$P_{c|s_0,h} = P(y \in D_0|s_0,h) = MP\left(y_r < \tau, |y_i| < y_r \tan\frac{\pi}{M}|s_0,h\right) = M\int_0^{\tau}\int_{-y_r\tan\frac{\pi}{M}}^{y_r\tan\frac{\pi}{M}} f_{y|s_0,h}(y|s_0,h)\,dy, \quad (14)$$

$$P_{c|s_1,h} = P(y \in \mathcal{D}_1|s_1,h) = P\left(y_r > \tau, |y_i| < y_r \tan\frac{\pi}{M}|s_1,h\right) = \int_{\tau}^{\infty}\int_{-y_r\tan\frac{\pi}{M}}^{y_r\tan\frac{\pi}{M}} f_{y|s_1,h}(y|s_1,h)\,dy, \text{ and} \quad (15)$$

respectively, by expressing the inner integrals using the Gaussian Q-function. In the above formulation, we have defined $y = y_r + jy_i$. Note that due to the circular symmetry of the constellation and the decision regions, the correct detection probabilities of the nonzero signals other than $s_1(t)$ are the same as in (15). Hence, the error probability can be expressed as in (10). □

Remark 1: For $M \geq 3$, we can easily observe that the region D_0 is an M-sided regular polygon[1] centered at the origin. Therefore, the nonzero signal $s_i(t)$ is detected if the received signal phase θ_y is closest to θ_i and y is outside the regular polygon for $M \geq 3$. For $M = 2$, $\mathcal{D}_0$ is an infinite rectangle.

Remark 2: The probability of error averaged over the realizations of the fading magnitude is obtained from $P_e = \int_0^{\infty} P_{e||h|}\,dF_{|h|}(|h|)$ where $F_{|h|}$ is the distribution function of the fading magnitude.

Remark 3: As SNR $\to 0$, we have $\alpha \to 0$, and hence

$$\zeta \to \begin{cases} \infty & \nu < \frac{M}{M+1} \\ -\infty & \nu > \frac{M}{M+1} \\ 0 & \nu = \frac{M}{M+1} \end{cases} \quad \text{and} \quad \tau \to \begin{cases} \infty & \nu < \frac{M}{M+1} \\ 0 & \nu \geq \frac{M}{M+1} \end{cases} . \quad (16)$$

If $\nu < \frac{M}{M+1}$, the threshold τ increases without bound as SNR vanishes. Therefore, $\mathcal{D}_0$ asymptotically becomes the complex plane and we have $P_{c|s_0,|h|} \to 1$, $P_{c|s_1,|h|} \to 0$, and $P_{e||h|} \to \nu$. On the other hand, if $\nu \geq \frac{M}{M+1}$, the decision region $\mathcal{D}_0$ vanishes and $P_{c|s_0,|h|} \to 0$. Indeed, for sufficiently small values of SNR for which $\zeta < 0$, we have $\tau = 0$. In such a case, $s_0(t)$ is never detected and the decision regions specialize to the decision regions of regular PSK modulation.

[1]A regular polygon is an n-sided convex polygon in which the sides are all the same length and are symmetrically placed about a common center.

Remark 4: As SNR $\to \infty$, it can be easily seen that $\tau \to \infty$. Hence, clearly $P_{c|s_0,|h|} \to 1$. By applying a change of variables with $\hat{x} = x - \alpha|h|$, we can express the correct detection probability of $s_1(t)$ in (11) as

$$P_{c|s_1,|h|} = \int_{\tau-\alpha|h|}^{\infty} \left(1 - 2Q\left(\sqrt{2}\,(\hat{x} + \alpha|h|)\tan\frac{\pi}{M}\right)\right)\frac{e^{-\hat{x}^2}}{\sqrt{\pi}}\,d\hat{x} \quad \overrightarrow{\text{SNR}\to\infty} \quad \int_{-\infty}^{\infty}\frac{e^{-\hat{x}^2}}{\sqrt{\pi}}\,d\hat{x} = 1. \tag{17}$$

The limiting value on the right hand side of (17) is obtained by noting that as $\alpha \to \infty$, $\tau - \alpha|h| = -\frac{\alpha|h|}{2} + \frac{1}{2\alpha|h|}\ln\left(\frac{M(1-\nu)}{\nu}\right) \to -\infty$ and $Q\left(\sqrt{2}\,(\hat{x} + \alpha|h|)\tan\frac{\pi}{M}\right) \to 0$. Therefore, not surprisingly, $P_{e|h|} \to 0$ as SNR increases.

Figure 1 plots the average error probability curves for 4-OOPSK signaling with different duty cycle values in the coherent Rayleigh fading channel with $E\{|h|^2\} = 1$. In ordinary M-PSK modulation, each symbol carries $\log_2 M$ bits. It is important to note that in M-OOPSK modulation, the maximum number of bits that can be carried by each symbol is equal to the entropy $H(\nu) = \nu\log_2(M/\nu) + (1-\nu)\log_2(1/(1-\nu))$ which decreases to zero as $\nu \to 0$. Hence, decreasing the duty cycle diminishes the data rates. For fair comparison, Fig. 1 plots the curves as a function of the SNR normalized by the entropy of the M-OOPSK source, giving the SNR per bit. It is observed from the figure that if the peakedness of the input signals is increased sufficiently (e.g., $\nu = 0.3, 0.1, 0.01$), significant improvements in error performance are achieved over the ordinary PSK (i.e., OOPSK with $\nu = 1$) performance. This is due to the fact that the minimum distance of the constellation increases with decreasing ν. We note that 4-OOPSK with $\nu = 0.8$ performs worse than regular 4-PSK. As expected from Remark 3, for $\nu < 0.8$, error probabilities approach ν as SNR $\to 0$. Fig. 2 plots the average error probabilities for 8-OOPSK signaling again as a function of the SNR per bit in the coherent Rayleigh fading channel with $E\{|h|^2\} = 1$. Similarly, it is observed that the error performance improves with decreasing duty cycle.

B. OOFSK

In this section, we assume that OOFSK signals are transmitted. The output of the bank of M demodulators is $\mathbf{y} = (y_1, y_2, \ldots, y_M)$. It is readily observed from (5) that conditioned on h and s_i, y_m is a proper complex Gaussian random variable with mean $E\{y_m|s_i,h\} = \alpha h e^{j\theta_i}\delta_{mi}$ and variance $var\{Y_m|s_i,h\} = E|n|^2 = 1$ where $\delta_{mi} = 1$ if $m = i$ and 0 otherwise. We assume that energy detection is employed. Hence, the detector observes $\mathbf{R} = (R_1, R_2, \ldots, R_M)$ where $R_m = |y_m|^2$ which gives the energy in the m^{th} frequency. Conditioned on s_i and $|h|$, $R_m = |y_m|^2$ is a chi-square random variable with two degrees of freedom and

the conditional probability density function of R_m is given by

$$f_{R_m|s_i,|h|}(R_m|s_i,|h|) = \begin{cases} e^{-(\alpha^2|h|^2+R_m)} I_0\left(2\sqrt{\alpha^2|h|^2 R_m}\right) & m = i \\ e^{-R_m} & m \neq i \end{cases} \tag{18}$$

where $m \in \{1,\ldots,M\}$ and $i \in \{0,1,\ldots,M\}$. Note that $\{R_i\}$ are i.i.d. random variables. The conditional joint distribution function of $\mathbf{R}$ is given by

$$f_{\mathbf{R}|s_i,|h|}(\mathbf{R}|s_i,|h|) = \begin{cases} e^{-\sum_{j=1}^{M} R_j} e^{-\alpha^2|h|^2} I_0\left(2\sqrt{R_i\alpha^2|h|^2}\right) & 1 \leq i \leq M \\ e^{-\sum_{j=1}^{M} R_j} & i = 0 \end{cases} \tag{19}$$

Again, MAP decision rule is used for the detection of the OOFSK signals. Hence, $s_i(t)$ is the detected signal if the following condition is satisfied:

$$p_i f_{\mathbf{R}|s_i,|h|}(\mathbf{R}|s_i,|h|) > p_j f_{\mathbf{R}|s_j,|h|}(\mathbf{R}|s_j,|h|) \quad \forall j \neq i \tag{20}$$

Note that we again have $p_i = \frac{\nu}{M}$ for $i \neq 0$ and $p_0 = 1-\nu$. The following proposition provides a simplified MAP decision rule and a closed-form expression for the error probability.

Proposition 2: The optimal MAP decision rule for OOFSK signaling in coherent fading channels is in the following form: $s_i(t)$ for $i \neq 0$ is detected if

$$R_i > R_j \ \forall j \neq i \quad \text{and} \quad R_i > \tau = \begin{cases} \frac{\left[I_0^{-1}(\xi)\right]^2}{4\alpha^2|h|^2} & \xi \geq 1 \\ 0 & \xi < 1 \end{cases}, \tag{21}$$

where $\xi = \frac{M(1-\nu)\, e^{\alpha^2|h|^2}}{\nu}$ and I_0^{-1} is the functional inverse of the zeroth order modified Bessel function of the first kind. No transmission and hence $s_0(t)$ is detected if $R_i < \tau \ \forall i$. The error probability of OOFSK modulation as a function of the instantaneous realization of the fading magnitude is

$$P_{e||h|} = 1 - ((1-\nu)P_{c|s_0,|h|} + \nu P_{c|s_1,|h|}) \tag{22}$$

where

$$P_{c|s_0,|h|} = (1-e^{-\tau})^M, \text{ and} \tag{23}$$

$$P_{c|s_1,|h|} = \sum_{n=0}^{M-1} \frac{(-1)^n}{n+1} \begin{pmatrix} M-1 \\ n \end{pmatrix} e^{-\frac{n}{n+1}\alpha^2|h|^2} Q_1\left(\sqrt{\frac{2}{n+1}}\alpha|h|, \sqrt{2(n+1)\tau}\right), \tag{24}$$

are the correct detection probabilities when $s_0(t)$ and $s_1(t)$, respectively, are the transmitted signals. In the above formulation, $Q_1(\cdot,\cdot)$ denotes the Marcum Q-function [19].

Proof: Using the prior probabilities and the conditional joint distribution function in (19), the detection rule in (20) can easily be simplified to that in (21) by noting that $I_0(x)$ is a monotonically increasing function of $x \geq 0$. Moreover, due to this monotonicity and the fact that $I_0(0) = 1$, the inverse function $I_0^{-1}(x)$ is well-defined for $x \geq 1$.

Having obtained the decision rules, we first express the correct detection probability conditioned on $s_1(t)$ being the transmitted signal and $|h|$:

$$\begin{aligned} P_{c|s_1,|h|} &= P(R_1 > R_2, \ldots, R_1 > R_M, R_1 > \tau \mid s_1, |h|) && (25)\\ &= \int_\tau^\infty P(R_1 > R_2, \ldots, R_1 > R_M \mid R_1 = x, s_1, |h|) f_{R_1|s_1,|h|}(x|s_1,|h|)dx && (26)\\ &= \int_\tau^\infty (1-e^{-x})^{M-1} e^{-(\alpha^2|h|^2+x)} I_0\left(2\sqrt{\alpha^2|h|^2 x}\right) dx && (27)\\ &= \sum_{n=0}^{M-1} (-1)^n \begin{pmatrix} M-1 \\ n \end{pmatrix} \int_\tau^\infty e^{-nx} e^{-(\alpha^2|h|^2+x)} I_0\left(2\sqrt{\alpha^2|h|^2 x}\right) dx && (28) \end{aligned}$$

where (27) follows by noting from (18) that $\{R_i\}_{i=2}^M$ are independent and identically distributed exponential random variables given that $s_1(t)$ is sent, and (28) is obtained by using the binomial expansion $(1-e^{-x})^{M-1} = \sum_{n=0}^{M-1} \begin{pmatrix} M-1 \\ n \end{pmatrix} (-1)^n e^{-nx}$. The Marcum Q-function is defined as $Q_1(\alpha,\beta) = \int_\beta^\infty x e^{-\frac{x^2+\alpha^2}{2}} I_0(\alpha x)dx$ [19]. By applying a change of variables, the integral in (28) can be expressed as a Marcum Q-function, leading to the expression in (24). Note that since the FSK signals are orthogonal, the correct detection probabilities for nonzero signals other than $s_1(t)$ are also equal to (24). When $s_0(t)$ is transmitted, the correct detection probability is

$$P_{c|s_0,|h|} = P(R_1 < \tau, , \ldots, R_M < \tau \mid s_0, |h|) = \left(\int_0^\tau e^{-x} dx\right)^M = (1-e^{-\tau})^M. \tag{29}$$

Finally, the error probability can be written as in (22). □

Remark 5: The probability of error averaged over the instantaneous realizations of the fading magnitude

is obtained from $P_e = \int_0^\infty P_{e||h|}\, dF_{|h|}|h|$ where $F_{|h|}$ is the distribution function of the fading magnitude $|h|$.

Remark 6: Conclusions similar to those in Remarks 3 and 4 in Section III-A can be drawn in this section as well. We again have

$$\lim_{\text{SNR}\to 0} \tau = \begin{cases} \infty & \nu < \frac{M}{M+1} \\ 0 & \nu \geq \frac{M}{M+1} \end{cases} \quad \text{and} \quad \lim_{\text{SNR}\to\infty} \tau = \infty. \tag{30}$$

The second limit in (30) can easily be shown by noting the fact that $I_0^{-1}(x) \geq \log x$. Using this fact, we have $\tau = \frac{\left[I_0^{-1}(\xi)\right]^2}{4\alpha^2|h|^2} \geq \frac{\log^2 \xi}{4\alpha^2|h|^2} = \frac{\left(\alpha^2|h|^2 + \log\frac{M(1-\nu)}{\nu}\right)^2}{4\alpha^2|h|^2} \to \infty$ as $\alpha \to \infty$. As a result, the correct detection probabilities show the same behavior as those in Remarks 3 and 4.

Figure 3 plots the average probability of error values of 16-OOFSK as a function of SNR per bit for different values of duty cycle parameter ν in the Rayleigh fading channel with $E\{|h|^2\} = 1$. Similarly as in Section III-A, OOFSK signaling with low duty cycle has superior performance in terms of error rates. From another perspective, if the duty cycle of the modulation is reduced, the same performance can be achieved at smaller SNR per bit values, improving the energy efficiency.

IV. Error Probability in Noncoherent Fading Channels

In this section, we consider the scenario in which neither the transmitter nor the receiver knows the instantaneous realizations of the fading coefficients. We consider a fast Rician fading environment and hence $\{h_k\}$ is a sequence of i.i.d. proper complex Gaussian random variables with mean $E\{h_k\} = d$ and variance $E\{|h_k|^2\} = \gamma^2$. It is assumed that channel statistics and hence the values of d and γ^2 are assumed to be known at the transmitter and receiver. Note that this model also represents scenarios in which training symbols are employed to facilitate channel estimation at the receiver, and the transmitter interleaves the data symbols for protection against error bursts. In such cases, d and γ^2 represent the channel estimate and the estimate error, respectively[2]. Moreover, due to interleaving, the data symbols experience independent fading.

A. OOPSK

Similarly as in Section III, MAP detection is employed at the detector. Hence, s_i is the detected signal if

[2]It should be noted that in training-based schemes, d and γ^2 are dependent on SNR.

$$p_i f_{y|s_i}(y|s_i) > p_j f_{y|s_j}(y|s_j) \quad \forall j \neq i \tag{31}$$

where the conditional probability density function in the absence of receiver channel knowledge is now given by

$$f_{y|s_i}(y|s_i) = \begin{cases} \frac{1}{\pi(\alpha^2\gamma^2+1)}\, e^{-\frac{|y-\alpha d e^{j\theta_i}|^2}{\alpha^2\gamma^2+1}} & 1 \leq i \leq M \\ \frac{1}{\pi}\, e^{-|y|^2} & i = 0 \end{cases}. \tag{32}$$

The following proposition describes the optimal decision regions and provides an expression for the error probability of OOPSK signaling in noncoherent Rician fading channels. Note that the results immediately specialize to Rayleigh fading channels when it is assumed that $d = 0$.

Proposition 3: The optimal decision regions for OOPSK signals when transmitted over noncoherent Rician fading channels are

$$\mathcal{D}_i = \left\{ y = |y|e^{j\theta_y} : \frac{2\pi(i-\frac{3}{2})}{M} \leq \theta_y \leq \frac{2\pi(i-\frac{1}{2})}{M} \text{ and } |y|^2 + \frac{2|d|}{\alpha\gamma^2}\,|y|\cos(\theta_y - \theta_i) > \tau \right\} \quad 1 \leq i \leq M,$$
$$\mathcal{D}_0 = \left\{ y = |y|e^{j\theta_y} : |y|^2 + \frac{2|d|}{\alpha\gamma^2}\,|y|\cos(\theta_y - \theta_i) < \tau \quad \forall i \neq 0 \right\} \tag{33}$$

where $\tau = \begin{cases} \zeta & \zeta \geq 0 \\ 0 & \zeta < 0 \end{cases}$ and $\zeta = \frac{|d|^2}{\gamma^2} + \left(1 + \frac{1}{\alpha^2\gamma^2}\right) \ln\left(\frac{M(1-\nu)}{\nu}\,(1+\alpha^2\gamma^2)\right)$. Furthermore, the error probability is given by

$$P_e = 1 - ((1-\nu)P_{c|s_0} + \nu P_{c|s_1}) \tag{34}$$

where

$$P_{c|s_0} = M\int_0^{\hat{\tau}} \left(1 - 2Q\left(\sqrt{2}x\tan\frac{\pi}{M}\right)\right)\frac{1}{\sqrt{\pi}}\,e^{-x^2}\,dx - M\int_{\hat{\tau}}^{\tilde{\tau}} \left(1 - 2Q\left(\sqrt{2}\sqrt{\tau - x^2 - \frac{2|d|}{\alpha\gamma^2}x}\right)\right)\frac{1}{\sqrt{\pi}}\,e^{-x^2}\,dx, \tag{35}$$

$$P_{c|s_1} = \int_{\hat{\tau}}^{\infty} \left(1 - 2Q\left(\frac{\sqrt{2}\,x\tan\frac{\pi}{M}}{\sqrt{1+\alpha^2\gamma^2}}\right)\right)\frac{1}{\sqrt{\pi(1+\alpha^2\gamma^2)}}\,e^{-\frac{(x-\alpha|d|)^2}{1+\alpha^2\gamma^2}}\,dx$$
$$- \int_{\hat{\tau}}^{\tilde{\tau}} \left(1 - 2Q\left(\frac{\sqrt{2}\sqrt{\tau - x^2 - \frac{2|d|}{\alpha\gamma^2}x}}{\sqrt{1+\alpha^2\gamma^2}}\right)\right)\frac{1}{\sqrt{\pi(1+\alpha^2\gamma^2)}}\,e^{-\frac{(x-\alpha|d|)^2}{1+\alpha^2\gamma^2}}\,dx \tag{36}$$

are the correct detection probabilities when $s_0(t)$ and $s_1(t)$, respectively, are the transmitted signals. In the

above integral expressions, $\hat{\tau} = \frac{1}{1+\tan^2\frac{\pi}{M}}\left(\sqrt{\frac{|d|^2}{\alpha^2\gamma^4}+\tau\left(1+\tan^2\frac{\pi}{M}\right)}-\frac{|d|}{\alpha\gamma^2}\right)$ and $\tilde{\tau} = \sqrt{\frac{|d|^2}{\alpha^2\gamma^4}+\tau}-\frac{|d|}{\alpha\gamma^2}$.

Proof: The decision rule (31) can easily be simplified to yield the following rule: s_i for $i \neq 0$ is the detected signal if

$$\Re(ye^{-j\theta_i}) > \Re(ye^{-j\theta_j}) \quad \forall j \neq i, 0 \quad \text{and} \quad |y|^2 + \frac{2|d|}{\alpha\gamma^2}\Re(ye^{-j\theta_i}) > \tau \tag{37}$$

where τ is defined in the proposition. The signal s_0 is the detected signal if

$$|y|^2 + \frac{2|d|}{\alpha\gamma^2}\Re(ye^{-j\theta_i}) < \tau \quad \forall i \neq 0. \tag{38}$$

Using the same arguments as in Section III, we obtain the above decision rules by assuming without loss generality that $d = |d|$. Otherwise, in all the decision rules, y must be replaced by $\tilde{y} = ye^{-\theta_d}$ where θ_d is the phase of fading mean d, which is known at the receiver. These detection rules lead to the decision regions given in (33).

The correct detection probability of a nonzero signal can be found by considering, without loss of generality, that $s_1(t)$ with phase $\theta_1 = 0$ is sent. Given that $s_1(t)$ is sent, the correct detection probability can be expressed as

$$P_{c|s_1} = P(y \in \mathcal{D}_1|s_1) = P\left(y_r > \hat{\tau}, |y_i| < y_r \tan\frac{\pi}{M} \mid s_1\right) - P\left(\hat{\tau} < y_r < \tilde{\tau}, |y_i| < \sqrt{\tau - y_r^2 - \frac{2|d|}{\gamma^2\alpha}y_r}|s_1\right) \tag{39}$$

where $y = y_r + jy_i$. We note that in the (y_r, y_i) plane, $\hat{\tau}$ is the horizontal axis value of the point at which the line $y_i = y_r \tan\frac{\pi}{M}$ and the circle $y_r^2 + y_i^2 + \frac{2|d|}{\alpha\gamma^2}y_r = \tau$ intersect, and $\tilde{\tau}$ is the value of the point at which the same circle intersects the horizontal axis. The correct detection probability for $s_0(t)$ is

$$P_{c|s_0} = MP\left(0 < y_r < \hat{\tau}, |y_i| < y_r \tan\frac{\pi}{M} \mid s_0\right) + MP\left(\hat{\tau} < y_r < \tilde{\tau}, |y_i| < \sqrt{\tau - y_r^2 - \frac{2|d|}{\alpha\gamma^2}y_r} \mid s_0\right). \tag{40}$$

The correct detection probability expressions in (35) and (36) are the integral representations of (40) and (39), respectively, obtained by representing the inner integrals by Q-functions. Finally, the error probability can be obtained from the correct detection probabilities as in (34). □

Remark 7: Note that $|y|^2 + \frac{2|d|}{\alpha\gamma^2}|y|\cos(\theta_y - \theta_i) < \tau$ defines a circular area. Therefore, $\mathcal{D}_0$ is the intersection of M circular regions.

Remark 8: It can again be easily verified that

$$\lim_{\text{SNR}\to 0} \tau = \begin{cases} \infty & \nu < \frac{M}{M+1} \\ 0 & \nu > \frac{M}{M+1} \end{cases} . \tag{41}$$

Therefore, similarly as in Remark 3, if $\nu < \frac{M}{M+1}$, $\lim_{\text{SNR}\to 0} P_e = \nu$. On the other hand, if $\nu > \frac{M}{M+1}$, decision region $\mathcal{D}_0$ vanishes with decreasing SNR.

Remark 9: As SNR $\to \infty$, we immediately observe that $\tau \to \infty$, and as a result, $\hat{\tau} \to \infty$, and $\tilde{\tau} \to \infty$. Asymptotically, $\mathcal{D}_0$ expands and becomes the complex plane. This leads us to conclude that $P_{c|s_0} \to 1$. We observe a different behavior from $P_{c|s_1}$. As SNR increases, the second integral in the expression of $P_{c|s_1}$ in (36) vanishes. After applying a change of variables with $\hat{x} = (x - \alpha|d|)/\sqrt{1+\alpha^2\gamma^2}$, the first integral in the expression of $P_{c|s_1}$in (36) can be written as

$$\int_{\frac{\hat{\tau}-\alpha|d|}{\sqrt{1+\alpha^2\gamma^2}}}^{\infty} \left(1 - 2Q\left(\sqrt{2}\tan\frac{\pi}{M}\left(\hat{x} + \frac{\alpha|d|}{\sqrt{1+\alpha^2\gamma^2}}\right)\right)\right) \frac{1}{\sqrt{\pi}} e^{-\hat{x}^2}\, d\hat{x}. \tag{42}$$

Taking the limit of (42) as SNR $\to \infty$ and hence $\alpha \to \infty$, we obtain

$$\lim_{\text{SNR}\to\infty} P_{c|s_1} = \int_{-\frac{|d|}{\gamma}}^{\infty} \left(1 - 2Q\left(\sqrt{2}\tan\frac{\pi}{M}\left(\hat{x} + \frac{|d|}{\gamma}\right)\right)\right) \frac{1}{\sqrt{\pi}} e^{-\hat{x}^2}\, d\hat{x} \stackrel{\text{def}}{=} P_{c,\infty|s_1}. \tag{43}$$

Note that $P_{c|s_1}$ does not approach to 1 as SNR $\to \infty$. Hence, we experience an error floor in noncoherent OOPSK signaling. The error floor is due to the presence of the multiplicative noise as a result of unknown fading. Even if the additive noise vanishes, errors are possible due to the distortion caused by unknown random phase shifts of fading. Note that $P_{c,\infty|s_1}$ depends only on the Rician factor $\mathsf{K} = \frac{|d|^2}{\gamma^2}$ and M. If $\gamma = 0$, then $\mathsf{K} = \infty$, and we have the unfaded Gaussian channel for which we can easily see that $P_{c,\infty|s_1} = 1$. Hence, no error floors exit in this case. If, on the other hand, $|d| = 0$ and hence $\mathsf{K} = 0$, we have the unknown Rayleigh fading channel for which $P_{c,\infty|s_1} = \frac{1}{M}$. Finally, as SNR $\to \infty$, we have $P_e \to \nu(1 - P_{c,\infty|s_1})$. Therefore, error floor decreases with decreasing duty cycle.

Fig. 4 plots the error probability curves for OOPSK signaling as a function of SNR per bit in the noncoherent Rician fading channel with Rician factor $\mathsf{K} = |d|^2/\gamma^2 = 10$. The plots are provided for constellation sizes of $M = 2, 4,$ and 8. Similarly as before, it is seen in all cases that the error performance improves as duty factor value decreases sufficiently. Note that for 8-OOPSK, even having a duty value of

$\nu = 0.8$ improves the performance with respect to the regular 8-PSK in the entire range of SNR per bit values considered in the graph. On the other hand, when $M = 2$, decreasing the duty cycle to $\nu = 0.8, 0.5$ or 0.3 does not provide gains with respect to the case of $\nu = 1$ unless SNR is high enough. As predicted, we observe error floors in all cases. We note that error floors decrease with decreasing constellation sizes and duty factors.

B. OOFSK

In this section, we consider OOFSK signaling. If $s_i(t)$ is transmitted, then y_m is a proper complex Gaussian random variable with mean $E\{y_m|s_i\} = \alpha d e^{j\theta_i}\delta_{mi}$ and variance $var\{y_m|s_i\} = \alpha^2\gamma^2\delta_{mi} + 1$ where $\delta_{mi} = 1$ if $m = i$ and zero otherwise. Since y_m is a complex Gaussian random variable, $R_m = |y_m|^2$ is chi-square distributed and the joint distribution function of the output vector $\mathbf{R}$ conditioned on $s_i(t)$ being transmitted is

$$f_{\mathbf{R}|s_i}(\mathbf{R}|s_i) = \begin{cases} e^{-\sum_{\substack{j=1 \\ j\neq i}}^{M} R_j} e^{-\frac{R_i+\alpha^2|d|^2}{1+\alpha^2\gamma^2}} I_0\left(\frac{2\sqrt{R_i\alpha^2|d|^2}}{1+\alpha^2\gamma^2}\right) & 1 \le i \le M \\ e^{-\sum_{j=1}^{M} R_j}, & i = 0 \end{cases}. \tag{44}$$

The following result provides the optimal detection rule and the error probability of OOFSK signaling in noncoherent Rician fading channels.

Proposition 4: The optimal MAP detection rule for OOFSK signaling over noncoherent Rician fading channels is given as follows: $s_i(t)$ for $i \neq 0$ is the detected signal if

$$R_i > R_j \quad \forall j \neq i \quad \text{and} \quad R_i > \tau = \begin{cases} \Phi^{-1}(\xi) & \xi \ge 1 \\ 0 & \xi < 1 \end{cases} \tag{45}$$

where

$$\Phi(x) = e^{\frac{\alpha^2\gamma^2 x}{1+\alpha^2\gamma^2}} I_0\left(\frac{2\sqrt{x\,\alpha^2|d|^2}}{1+\alpha^2\gamma^2}\right) \text{ and } \xi = \frac{M(1-\nu)}{\nu}(1+\alpha^2\gamma^2)\, e^{\frac{\alpha^2|d|^2}{1+\alpha^2\gamma^2}}. \tag{46}$$

$s_0(t)$ is the detected signal if $R_i < \tau\ \forall i$. The probability of error is

$$P_e = 1 - ((1-\nu)P_{c|s_0} + \nu P_{c|s_1}) \tag{47}$$

where

$$P_{c|s_0} = \left(1 - e^{-\tau}\right)^M \quad \text{and,} \tag{48}$$

$$P_{c|s_1} = \sum_{n=0}^{M-1} (-1)^n \begin{pmatrix} M-1 \\ n \end{pmatrix} \frac{e^{-\frac{n\alpha^2|d|^2}{n(1+\alpha^2\gamma^2)+1}}}{n(1+\alpha^2\gamma^2)+1} Q_1\left(\sqrt{\frac{2\alpha^2|d|^2}{(1+\alpha^2\gamma^2)[n(1+\alpha^2\gamma^2)+1]}}, \sqrt{\frac{2[n(1+\alpha^2\gamma^2)+1]\tau}{(1+\alpha^2\gamma^2)}}\right) \tag{49}$$

are the correct detection probabilities when $s_0(t)$ and $s_1(t)$, respectively, are the transmitted signals.

Proof: The MAP decision rule in (45) can be easily obtained by using the conditional density function expression in (44) in the general MAP detection rule $p_i f_{\mathbf{R}|s_i}(\mathbf{R}|s_i) > p_j f_{\mathbf{R}|s_j}(\mathbf{R}|s_j)$ for all $j \neq i$. Since Φ is a monotonically increasing function and $\Phi(0) = 1$, the functional inverse $\Phi^{-1}(x)$ is well-defined for $x \geq 1$. If $s_1(t)$ is assumed to be transmitted, then, similarly as in the proof of Proposition 2, the probability of correct detection is

$$P_{c|s_1} = P\left(R_1 > R_2, \ldots, R_1 > R_M, R_1 > \tau \mid s_1\right) \tag{50}$$

$$= \sum_{n=0}^{M-1} (-1)^n \begin{pmatrix} M-1 \\ n \end{pmatrix} \int_\tau^\infty \frac{1}{1+\alpha^2\gamma^2} e^{-\frac{[n(1+\alpha^2\gamma^2)+1]x+\alpha^2|d|^2}{1+\alpha^2\gamma^2}} I_0\left(\frac{2\alpha|d|\sqrt{x}}{1+\alpha^2\gamma^2}\right) dx. \tag{51}$$

$$= \sum_{n=0}^{M-1} (-1)^n \begin{pmatrix} M-1 \\ n \end{pmatrix} \frac{e^{-\frac{n\alpha^2|d|^2}{(n(1+\alpha^2\gamma^2)+1)}}}{n(1+\alpha^2\gamma^2)+1} \int_{[n(1+\alpha^2\gamma^2)+1]\tau}^\infty \frac{e^{-\frac{x+\alpha^2|d|^2}{1+\alpha^2\gamma^2}}}{1+\alpha^2\gamma^2} I_0\left(\frac{2\alpha|d|\sqrt{x}}{1+\alpha^2\gamma^2}\right) dx. \tag{52}$$

The integral in (52) can be expressed as a Marcum Q-function and we obtain (49). When no signal is transmitted, the probability of correct detection is

$$P_{c|s_0} = P\left(R_1 < \tau, \ldots, R_M < \tau \mid s_0\right) = \left(\int_0^\tau e^{-x} dx\right)^M = \left(1 - e^{-\tau}\right)^M. \tag{53}$$

Finally, the probability of error is given as in (47). □

Remark 10: The Marcum Q-function has the following bounds when $\beta > \alpha > 0$ [19]:

$$\frac{\beta}{\beta+\alpha} e^{-\frac{(\beta+\alpha)^2}{2}} \leq Q_1(\alpha, \beta) \leq \frac{\beta}{\beta-\alpha} e^{-\frac{(\beta-\alpha)^2}{2}}. \tag{54}$$

Hence, in (49), when $\frac{\beta}{\alpha} = \sqrt{\frac{[n(1+\alpha^2\gamma^2)+1]^2\tau}{\alpha^2|d|^2}} > 1$, we can obtain bounds expressed using exponential functions rather than the Marcum Q-functions.

If $|d| = 0$, we have the Rayleigh fading channel. In this case, error probability expression simplifies immediately because $Q_1(0, \beta) = e^{-\beta^2/2}$.

Remark 11: We can easily show that

$$\lim_{\text{SNR}\to 0} \tau = \begin{cases} \infty & \nu < \frac{M}{M+1} \\ 0 & \nu > \frac{M}{M+1} \end{cases} \quad \text{and} \quad \lim_{\text{SNR}\to\infty} \tau = \infty. \tag{55}$$

From the first limit in (55), we note that if $\nu < \frac{M}{M+1}$, we again have $P_e \to \nu$ as SNR $\to 0$.

Let us now consider the second limit in (55). From (45), we have $\Phi(\tau) = \xi$ for large SNR. Using the fact that $I_0(x) \leq e^x \ \forall x \geq 0$, we have $\xi \leq e^{\frac{\alpha^2\gamma^2\tau + 2\sqrt{\alpha^2|d|^2\tau}}{1+\alpha^2\gamma^2}}$. By taking the logarithm of both sides of this inequality, we can easily show the second limit in (55). Therefore, we can easily see that $P_{c|s_0} \to 1$ as SNR increases. Next, we consider $P_{c|s_1}$. In the correct detection probability expression in (49), the terms in the summation, for which $n \neq 0$, approach to zero with increasing SNR due to the presence of $(n(1+\alpha^2\gamma^2)+1)$ in the denominator and the fact that Marcum Q-function, being a probability, is upper bounded by 1. When $n = 0$, the term in the summation is $Q_1\left(\sqrt{\frac{2\alpha^2|d|^2}{1+\alpha^2\gamma^2}}, \sqrt{\frac{2\tau}{1+\alpha^2\gamma^2}}\right)$. Since $I_0(x) \geq 1 \ \forall x \geq 0$, we have $e^{\frac{\alpha^2\gamma^2\tau}{1+\alpha^2\gamma^2}} \leq \xi$ from which we can easily observe, by taking the logarithm of both sides, that τ increases at most logarithmically with increasing α. Therefore, as $\alpha \to \infty$, $Q_1\left(\sqrt{\frac{2\alpha^2|d|^2}{1+\alpha^2\gamma^2}}, \sqrt{\frac{2\tau}{1+\alpha^2\gamma^2}}\right) \to Q_1\left(\sqrt{\frac{2|d|^2}{\gamma^2}}, 0\right) = 1$. Hence, as SNR $\to \infty$, $P_{c|s_1} \to 1$, and hence $P_e \to 0$. Therefore, unlike the OOPSK case, we do not have error floors in this case due to the immunity of OOFSK with energy detection to random phase rotations of fading.

Fig. 5 provides the error rates of 16-OOFSK over the noncoherent Rayleigh fading channel while Fig. 6 gives the error rates in the noncoherent Rician channel with $\mathsf{K} = 5$. We observe that unlike the OOPSK case, OOFSK performance is free of error floors at high SNRs. As SNR decreases, we see that $P_e \to \nu$ for the cases in which $\nu < M/(M+1)$. Moreover, we note that modulations with $\nu < 1$ perform better than that with $\nu = 1$ at low SNRs. However, at high SNR levels, gains are realized if the duty factor is sufficiently small.

V. Random Coding Error Exponents of Peaky Signaling

In [17], Gallager derived upper bounds on the probability of error that can be achieved by block codes on general discrete-time memoryless channels. Using an ensemble of codebooks where each letter of each codeword is chosen independently of all other letters with a certain probability distribution, it is shown in [17] that for any rate R less than the channel capacity, the probability of error can be upper bounded by $P_e \leq Be^{-NE(R)}$ where B is a constant, N is the codeword length, and $E(R)$ is the random coding error

exponent. $E(R)$ provides the interactions between the probability of error, channel coding, data rates, and the signal-to-noise ratio (SNR). The random coding error exponent is obtained from

$$E(R) = \sup_{0 \leq \rho \leq 1} E_0(\rho) - \rho R \tag{56}$$

where

$$E_0(\rho) = -\log \int_y \left(\frac{\nu}{M} \sum_{i=1}^{M} f_{y|s_i}(y|s_i)^{\frac{1}{1+\rho}} + (1-\nu) f_{y|s_0}(y|s_0)^{\frac{1}{1+\rho}} \right)^{1+\rho} \mathrm{d}y \tag{57}$$

for OOPSK modulation and

$$E_0(\rho) = -\log \int_{\mathbf{R}} \left(\frac{\nu}{M} \sum_{i=1}^{M} f_{\mathbf{R}|s_i}(\mathbf{R}|s_i)^{\frac{1}{1+\rho}} + (1-\nu) f_{\mathbf{R}|s_0}(\mathbf{R}|s_0)^{\frac{1}{1+\rho}} \right)^{1+\rho} \mathrm{d}\mathbf{R} \tag{58}$$

for OOFSK modulation. Note that for coherent fading channels, $f_{y|s_i}$ and $f_{\mathbf{R}|s_i}$ are replaced by $f_{y|s_i,h}$ and $f_{\mathbf{R}|s_i,|h|}$, respectively. In the coherent case, $E(R,h)$ is also a function of h and the average error exponent is obtained from $E_h\{E(R,h)\}$ where E_h denotes the expectation with respect to h.

We have numerically solved the optimization problem in (56) and we now present the results for the random coding error exponents of OOPSK and OOFSK modulations in both coherent and noncoherent fading channels. We first focus on noncoherent fading channels. Fig. 7 plots the error exponents as a function of data rates R of 16-OOPSK in the noncoherent Rician fading channel with $\mathsf{K} = 1$ when $\text{SNR} = 1$. Fig. 8 is a closer look at the exponents at high rates. From these figures, we note that OOPSK with duty cycles $\nu = 0.8, 0.6,$ and 0.4 have higher error exponents with respect to that of regular PSK (i.e., $\nu = 1$) over the entire range of rate values. While signaling with $\nu = 0.6$ provides the highest exponents for low rates, error exponents of $\nu = 0.4$ eventually exceeds those of $\nu = 0.6$ at high rates as evidenced in Fig. 8. We further observe that the error performance is relatively poor when $\nu = 0.1$. Fig. 9 provides the error exponents in the same channel when $\text{SNR} = 0.1$. We note that at this low value of the SNR, signaling with low duty cycle (e.g., $\nu = 0.2$ or 0.1) results in improved performance at high rates in contrast to the behavior at $\text{SNR} = 1$. Fig. 10 plots the error exponents of 2-OOFSK in the noncoherent Rayleigh fading channel when $\text{SNR} = 1$. In this figure, we see that signaling with duty cycle less than 1 improves the performance for all rates. Among the parameters considered in the figure, $\nu = 0.2$ gives the highest exponents at all rates. We have quiet different results when coherent channels are considered. Fig. 11 gives the error exponents

of 16-OOPSK in the coherent Rician fading channel with $\mathsf{K} = 1$. We immediately observe that in general signaling with duty cycle less than 1 degrades the performance. Improvements over the case of $\nu = 1$ is possible only at high rates when $\nu = 0.8$. Hence, the gains in error performance that we observe in uncoded systems are not realized in coded systems when error exponents are considered.

VI. Conclusion

We have studied the error performance of peaky signaling over fading channels. We have considered two modulation formats: OOPSK and OOFSK. We have initially concentrated on uncoded systems. We have found the optimal MAP decision rules and obtained analytical error probability expressions for OOPSK and OOFSK transmissions over both coherent and noncoherent fading channels. Through numerical results, we have seen that error performance improves if the peakedness of the signaling schemes are sufficiently increased. For fixed error probabilities, substantial gains in terms of SNR per bit are realized, making the peaky signaling schemes energy efficient. Since decreasing the duty cycle diminishes the communication rates, information-theoretic inspired OOPSK and OOFSK emerge as energy-efficient modulation techniques well-suited for low data rate applications. We have also analyzed the performance of coded systems. We have numerically obtained the random coding error exponents of both OOPSK and OOFSK. In noncoherent channels, we have seen improvements in the performance if the duty cycles are less than 1. On the other hand, we have observed that operating with low duty cycles in coded systems in general degrades the performance in coherent fading channels. This paper has mainly considered single-user, single-antenna systems. Recently, we have considered in [20] the reception of OOFSK signals using multiple antennas at the receiver. Results similar to those reported in this paper are noted for the error performance. Future work includes the design of peaky signaling schemes for multiple-input multiple-output (MIMO) systems. Note that since signaling with a duty cycle decreases collisions in a multiuser environment, the analysis of the impact of peaky signaling on the design of medium access algorithms is also a future research direction.

References

[1] I. Abou-Faycal, M. D. Trott, and S. Shamai (Shitz), "The capacity of discrete-time memoryless Rayleigh fading channels," *IEEE Trans. Inform. Theory*, vol. 47, pp. 1290-1301, May 2001.

[2] T. H. Chan, S. Hranilovic and F. R. Kschischang, "Capacity-achieving probability measure for conditionally Gaussian channels with bounded inputs," *IEEE Trans. Inform. Theory*, vol. 51, pp. 2073-2088, June 2005.

[3] J. Huang and S. P. Meyn, “Characterization and computation of optimal distributions for channel coding,” *IEEE Trans. Inform. Theory*, vol. 51, pp. 2336-2351, July 2005.

[4] M. Katz and S. Shamai (Shitz), “On the capacity-achieving distribution of the discrete-time non-coherent and partially-coherent AWGN channels,” *IEEE Trans. Inform. Theory*, vol. 50, pp. 2257-2270, Oct. 2004.

[5] S. Verdú, “Spectral efficiency in the wideband regime,” *IEEE Trans. Inform. Theory*, vol. 48, pp. 1319-1343, June 2002.

[6] M. C. Gursoy, H. V. Poor, and S. Verdú, “The noncoherent Rician fading channel – Part I : Structure of the capacity-achieving input,” *IEEE Trans. Wireless Commun.*, vol. 4, no. 5, pp. 2193-2206, Sept. 2005.

[7] M. C. Gursoy, H. V. Poor, and S. Verdú, “The noncoherent Rician fading channel – Part II : Spectral efficiency in the low-snr regime,” *IEEE Trans. Wireless Commun.*, vol. 4, no. 5, pp. 2207 - 2221, Sept. 2005.

[8] M. Médard and R. G. Gallager, “Bandwidth scaling for fading multipath channels,” *IEEE Trans. Inform. Theory*, vol. 48, pp. 840-852, Apr. 2002.

[9] V. G. Subramanian and B. Hajek, “Broad-band fading channels: signal burstiness and capacity,” *IEEE Trans. Inform. Theory*, vol. 48, pp. 809-827, Apr. 2002.

[10] I. E. Telatar and D. N. C. Tse, “Capacity and mutual information of wideband multipath fading channels,” *IEEE Trans. Inform. Theory*, vol. 46, pp. 1384-1400, July 2000.

[11] C. Luo, M. Medard, and L. Zheng, “On approaching wideband capacity using multitone FSK”, *IEEE Jour. Select. Areas Commun.*, vol. 23, no. 9, pp. 1830 - 1838, Sept. 2005.

[12] D. Lun, M. Medard, and I. C. Abou-Faycal, “On the performance of peaky capacity-achieving signaling on multipath fading channels”, *IEEE Jour. Select. Areas Commun.*, vol. 24, no. 8, pp. 1647 - 1661, Aug. 2006.

[13] M. C. Gursoy, “Error exponents and cutoff rate for noncoherent Rician fading channels,” Proceedings of the IEEE International Conference on Communications, Istanbul, Turkey, June, 11-15, 2006.

[14] J. Huang, S. P. Meyn and M. Medard, “Error exponents for channel coding with application to signal constellation design,” *IEEE Trans. Inform. Theory*, vol. 51, pp. 2336-2351, July 2005.

[15] X. Wu and R. Srikant, “MIMO channels in the low-SNR regime: Communication rate, error exponent, and signal peakiness,” *IEEE Trans. Inform. Theory*, vol. 53, pp. 1290-1309, Apr. 2007.

[16] S. Ray, M. Medard, and L. Zheng, “On noncoherent MIMO channels in the wideband regime: Capacity and reliability,” *IEEE Trans. Inform. Theory*, vol. 53, pp. 1983-2009, June 2007.

[17] R. G. Gallager, “A simple derivation of the coding theorem and some applications,” *IEEE Trans. Inform. Theory*, vol. 11, pp. 3-18, Jan. 1965.

[18] M. C. Gursoy, H. V. Poor, S. Verdú, “On-Off frequency-shift keying for wideband fading channels” *EURASIP Journal on Wireless Communications and Networking*, 2006.

[19] M. K. Simon and M.-S. Alouni, ”A unified approach to the performance analysis of digital communication over generalized fading channels”, *Proc. of the IEEE*, vol. 86, no. 9, pp. 1860-1877, Sept. 1998

[20] Q. Wang and M.C. Gursoy, “Performance analysis for multichannel reception of OOFSK signaling,” Proc. of the IEEE Wireless Communications and Networking Conference (WCNC), Hong Kong, 2007.

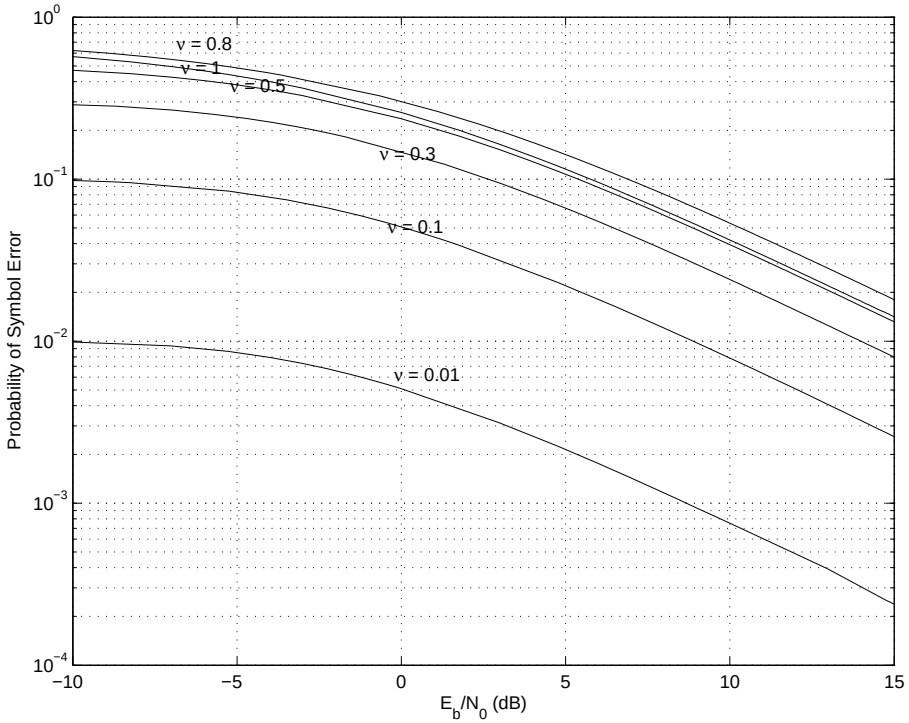

Fig. 1. Probability of symbol error vs. E_b/N_0 for 4-OOPSK signaling with different duty factor values, ν, in coherent Rayleigh fading channels with $E\{|h|^2\} = 1$.

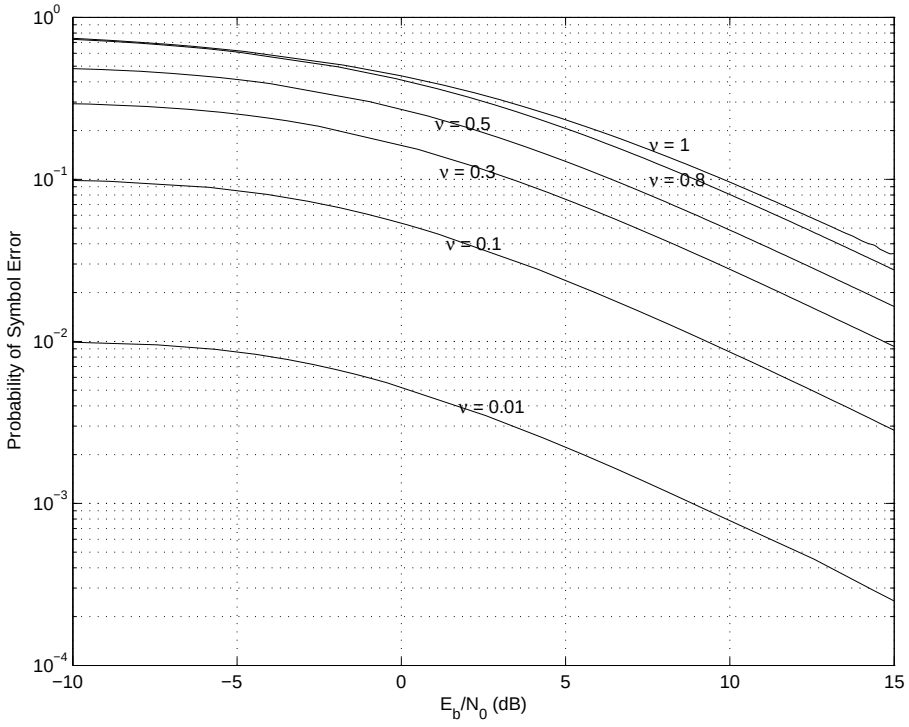

Fig. 2. Probability of symbol error vs. E_b/N_0 for 8-OOPSK signaling with different duty factor values, ν, in coherent Rayleigh fading channels with $E\{|h|^2\} = 1$.

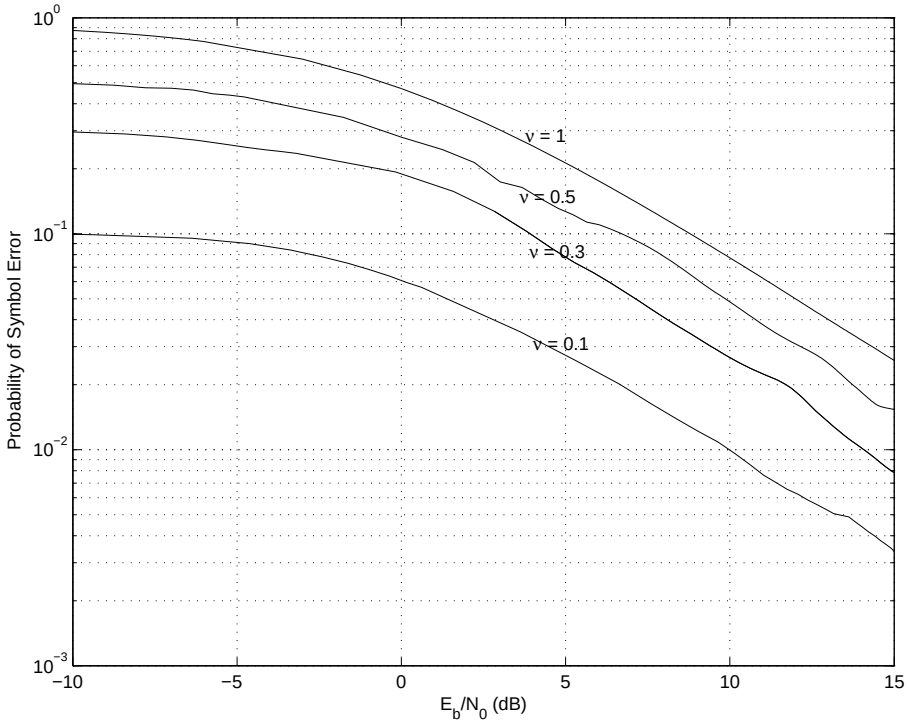

Fig. 3. Probability of error of 16-OOFSK in the coherent Rayleigh fading channel with $E\{|h|^2\} = 1$. The duty factor values are $\nu = 1, , 0.5, 0.3$ and 0.1.

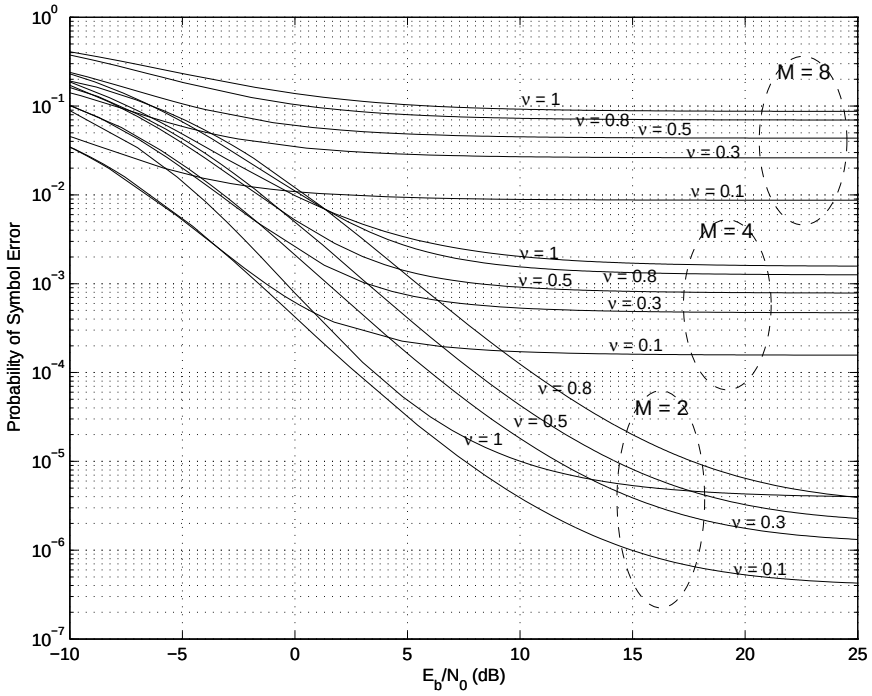

Fig. 4. Probability of symbol error vs. E_b/N_0 for OOPSK signaling with duty factor values $\nu = 1, 0.8, 0.5, 0.3, 0.1$ and constellation sizes $M = 2, 4, 8$ in the noncoherent Rician fading channel with Rician factor $\mathsf{K} = |d|^2/\gamma^2 = 10$.

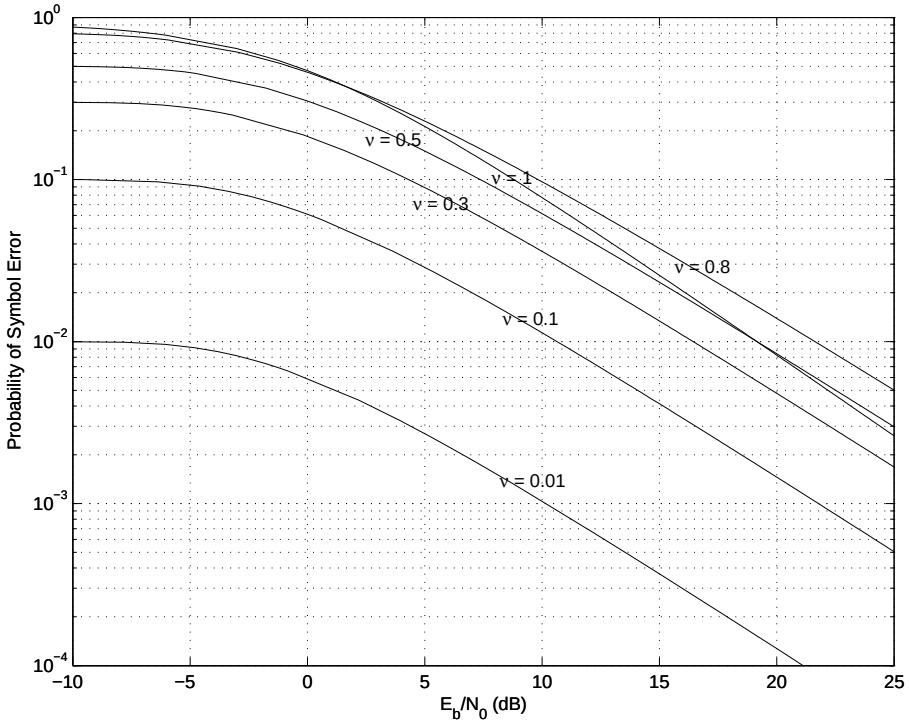

Fig. 5. Error probability of 16-OOFSK in the noncoherent Rayleigh fading channel with duty factors $\nu = 1, 0.8, 0.5, 0.3, 0.1,$ and 0.01.

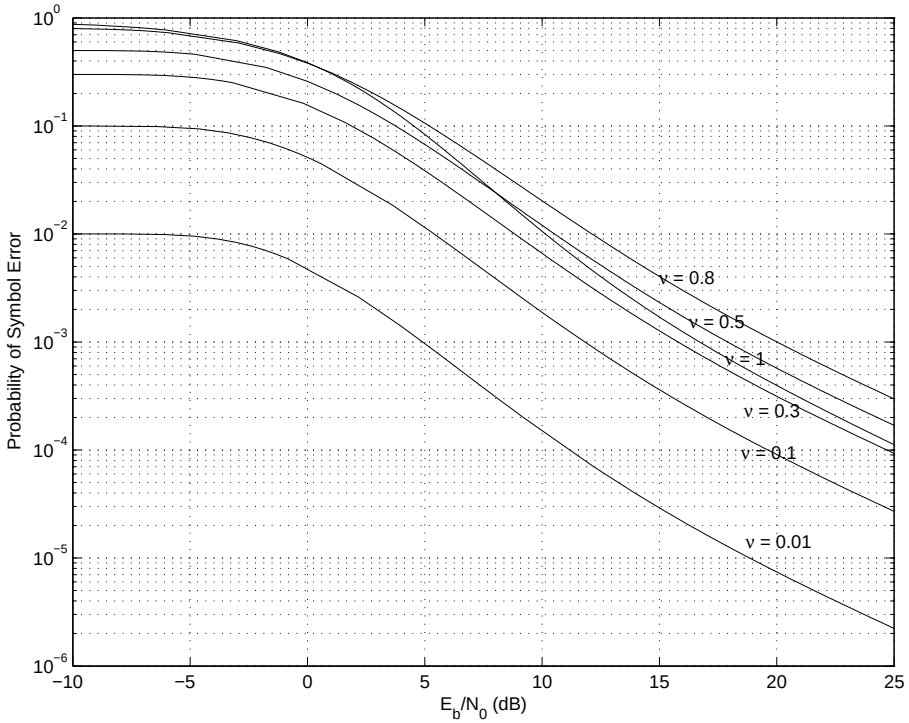

Fig. 6. Error probability of 16-OOFSK in the noncoherent Rician fading channel with Rician factor $\mathsf{K} = \frac{|d|^2}{\gamma^2} = 5$. The duty factor values are $\nu = 1, 0.8, 0.5, 0.3, 0.1,$ and 0.01.

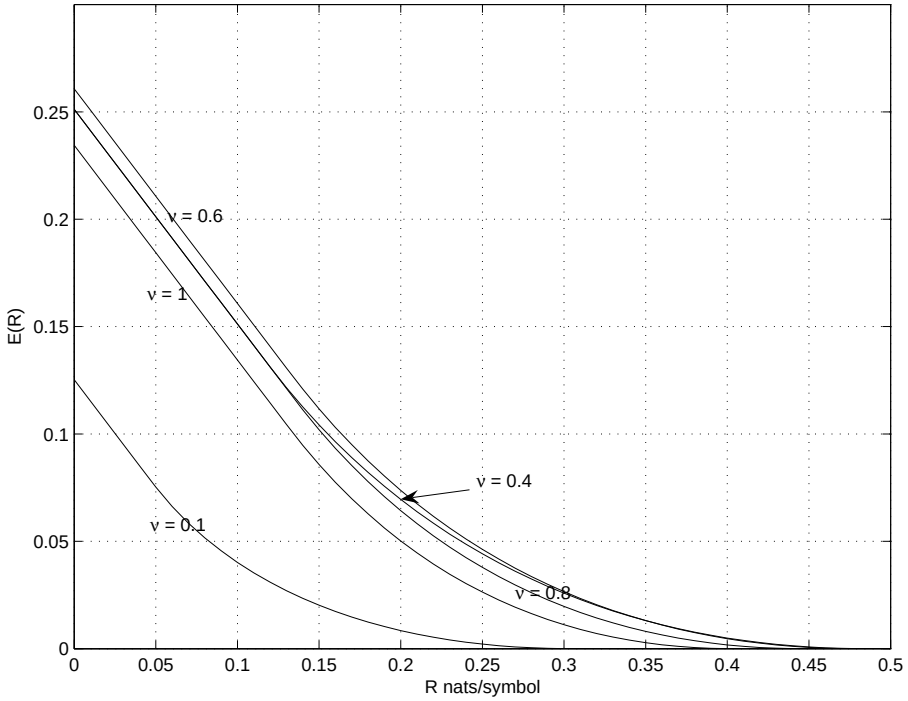

Fig. 7. Random coding error exponent of 16-OOPSK in the noncoherent Rician fading channel with Rician factor $\mathsf{K} = \frac{|d|^2}{\gamma^2} = 1$. The duty factor values are $\nu = 1, 0.8, 0.6, 0.4, 0.1$. SNR $= 1$.

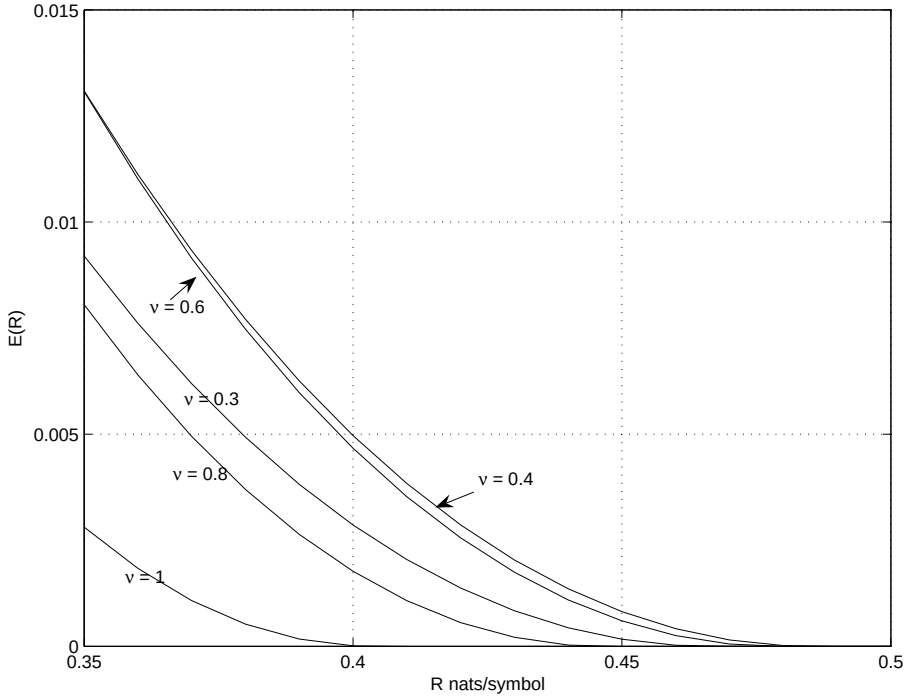

Fig. 8. Random coding error exponent of 16-OOPSK in the noncoherent Rician fading channel with Rician factor $\mathsf{K} = \frac{|d|^2}{\gamma^2} = 1$. The duty factor values are $\nu = 1, 0.8, 0.6, 0.4, 0.3$. SNR $= 1$.

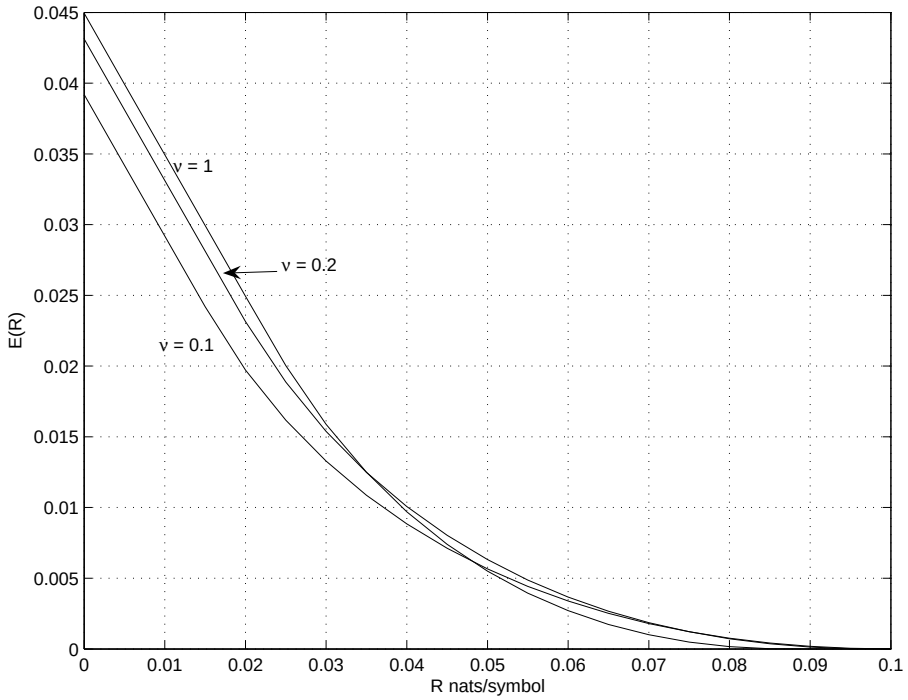

Fig. 9. Random coding error exponent of 16-OOPSK in the noncoherent Rician fading channel with Rician factor $\mathsf{K} = \frac{|d|^2}{\gamma^2} = 1$. The duty factor values are $\nu = 1, 0.2, 0.1$. SNR $= 0.1$.

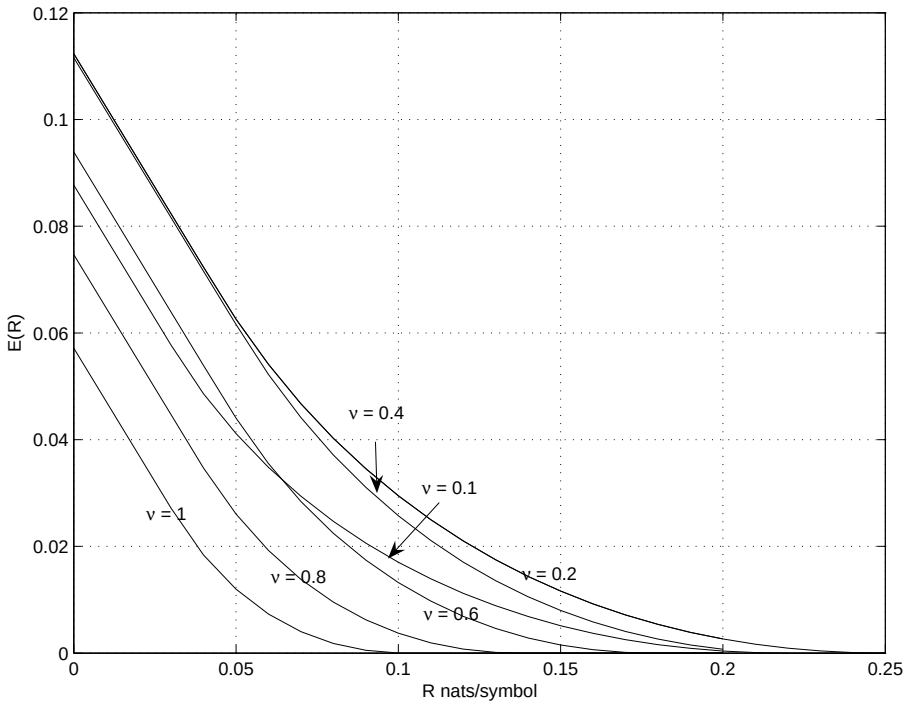

Fig. 10. Random coding error exponent of 2-OOFSK in the noncoherent Rayleigh fading channel. The duty factor values are $\nu = 1, 0.8, 0.6, 0.4, 0.2, 0.1$. SNR $= 1$.

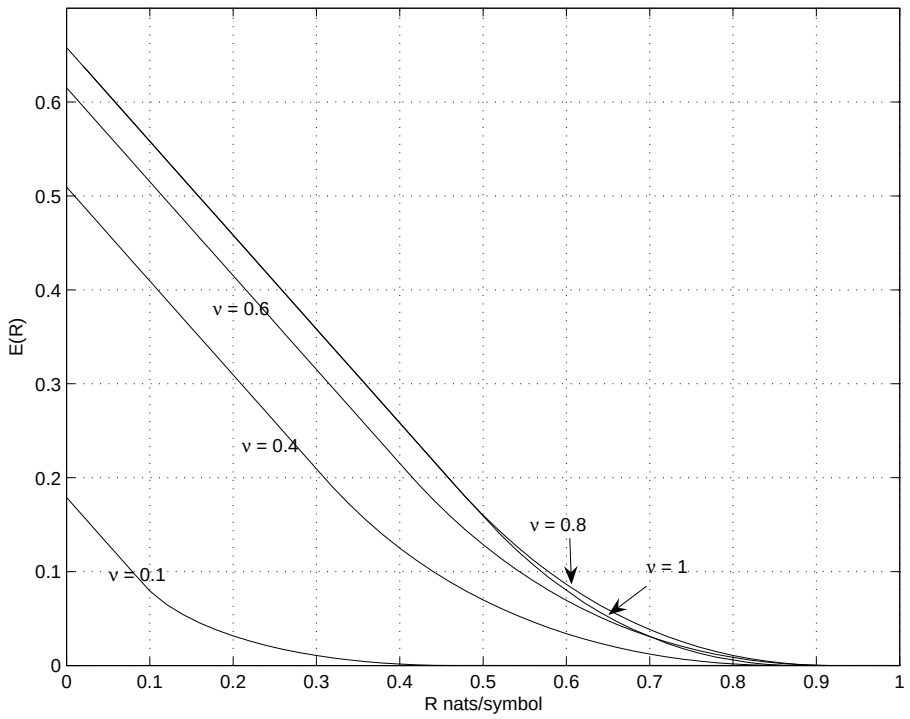

Fig. 11. Random coding error exponent of 16-OOPSK in the coherent Rician fading channel with Rician factor $\mathsf{K} = 1$. The duty factor values are $\nu = 1, 0.8, 0.6, 0.4, 0.1$. SNR $= 1$.